

An Integrated Device for the Solar-Driven Electrochemical Conversion of CO<sub>2</sub> to CO

*Original*

An Integrated Device for the Solar-Driven Electrochemical Conversion of CO<sub>2</sub> to CO / Sacco, A., Speranza, R., Savino, U., Zeng, J., Farkhondehfar, M.A., Lamberti, A., Chiodoni, A., Pirri, C.F.. - In: ACS SUSTAINABLE CHEMISTRY & ENGINEERING. - ISSN 2168-0485. - ELETTRONICO. - 8:20(2020), pp. 7563-7568. [10.1021/acssuschemeng.0c02088]

*Availability:*

This version is available at: 11583/2837210 since: 2020-06-25T19:56:23Z

*Publisher:*

AMER CHEMICAL SOC

*Published*

DOI:10.1021/acssuschemeng.0c02088

*Terms of use:*

This article is made available under terms and conditions as specified in the corresponding bibliographic description in the repository

*Publisher copyright*

GENERICO -- per es. Nature : semplice rinvio dal preprint/submitted, o postprint/AAM [ex default]

The original publication is available at <https://pubs.acs.org/doi/10.1021/acssuschemeng.0c02088> / <http://dx.doi.org/10.1021/acssuschemeng.0c02088>.

(Article begins on next page)

# 1 An Integrated Device for the Solar-Driven Electrochemical 2 Conversion of CO<sub>2</sub> to CO

3 Adriano Sacco,\* Roberto Speranza, Umberto Savino, Juqin Zeng, M. Amin Farkhondehfal,  
4 Andrea Lamberti,\* Angelica Chiodoni, and Candido F. Pirri



Cite This: <https://dx.doi.org/10.1021/acssuschemeng.0c02088>



Read Online

ACCESS |



Metrics & More



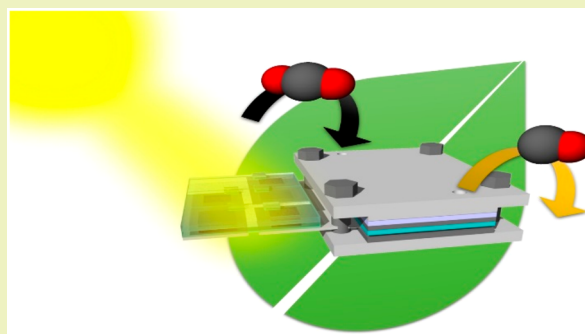
Article Recommendations



Supporting Information

5 **ABSTRACT:** The conversion of carbon dioxide into value-added  
6 products using sunlight, also called artificial photosynthesis, represents a  
7 remarkable and sustainable approach to store solar energy, transforming  
8 it into chemical energy. There are mainly two strategies to carry out this  
9 process: the photocatalytic reduction of carbon dioxide (CO<sub>2</sub>) or the  
10 photovoltaic-powered electrochemical reduction of CO<sub>2</sub>. Herein, we  
11 focus on the latter route, i.e., the development of a device coupling a  
12 solar cell to an electrochemical reactor for CO<sub>2</sub> reduction. Different  
13 literature works demonstrated the possibility to achieve such a coupling,  
14 but no evidence of a real integration between the two systems has been  
15 given up to now. In this work, we present an integrated device  
16 constituted by a dye-sensitized solar module (based on a mesoporous  
17 titanium dioxide photoanode) and an electrochemical cell (based on a copper–tin  
18 cathode). The integration of the two systems is  
19 accomplished through a common platinum-based electrode, which acts either as a cathode for the photovoltaic module and as an  
20 anode for the electrochemical reactor. The integrated system was characterized by a stable current of 3.6 mA under continuous solar  
21 irradiation, enabling the production of 80 mmol of carbon monoxide per day, with a solar-to-fuel efficiency equal to 0.97%.

22 **KEYWORDS:** Artificial photosynthesis, Integrated device, Dye-sensitized solar cells, Photovoltaic module, CO<sub>2</sub> reduction reaction,  
23 Electrochemical conversion



## 23 ■ INTRODUCTION

24 Artificial photosynthesis, i.e., the conversion of solar energy to  
25 chemical energy, mimicking the plants' process of natural  
26 photosynthesis, has attracted a lot of interest in the scientific  
27 community.<sup>1</sup> Essentially, two types of artificial photosynthesis  
28 processes are studied by scientists, namely, photocatalytic  
29 water splitting,<sup>2</sup> i.e., the conversion of water into oxygen and  
30 hydrogen, and the solar-driven carbon dioxide reduction  
31 reaction (CO<sub>2</sub>RR), i.e., the conversion of CO<sub>2</sub> to carbon-  
32 based value-added products.<sup>3</sup> The latter is of particular interest  
33 because it would allow attaining a triple goal: (1) storing the  
34 excess energy coming from the Sun that is not put in the  
35 electric grid,<sup>4</sup> (2) reduction of atmospheric CO<sub>2</sub>, i.e., the major  
36 greenhouse gas, which can be used as a raw material,<sup>5</sup> and (3)  
37 production of valuable chemicals.<sup>6</sup>

38 Apart from systems employing photoelectrodes,<sup>7–9</sup> there are  
39 different examples in the literature dealing with solar-driven  
40 CO<sub>2</sub> electroreduction obtained by coupling a photovoltaic  
41 (PV) device with an electrochemical cell (EC).<sup>10–17</sup> As an  
42 example, Kauffman et al. used a commercial 6 V Si solar  
43 module to power a two-chamber electrochemical reactor with a  
44 gold (Au) cathode and a platinum (Pt) anode which was able  
45 to produce more than 400 L/(g<sub>Au</sub> h) of carbon monoxide  
46 (CO) with a selectivity of about 96%.<sup>10</sup> Schreier and co-

workers employed three series-connected perovskite solar cells 47  
to power a single-chamber electrolyzer with a Au cathode<sup>11</sup> 48  
and studied a triple-junction GaInP/GaInAs/Ge PV device 49  
coupled with a dual-chamber EC based on a SnO<sub>2</sub>-coated CuO 50  
cathode and anode.<sup>12</sup> In both cases, a selectivity toward CO 51  
larger than 80% was reached, with solar-to-CO efficiencies 52  
equal to 6.5% and 13.4% for perovskite- and triple-junction- 53  
based systems, respectively. A 1.4% solar-to-formate efficiency 54  
was obtained by White et al. employing a poly-Si solar panel 55  
and a three-cell electrolyzer stack composed of indium (In)- 56  
based cathodes and iridium oxide (IrO<sub>2</sub>)-based anodes.<sup>13</sup> 57  
Moreover, hydrocarbons and oxygenates can be produced by 58  
solar-driven CO<sub>2</sub> reduction,<sup>16</sup> with a conversion efficiency 59  
larger than 5% by using a III–V/Si tandem PV cell and a two- 60  
chamber reactor with a nanostructured copper–silver (Cu– 61  
Ag) bimetallic cathode and IrO<sub>2</sub> anode. A lower solar-to- 62  
hydrocarbons efficiency equal to 2.3% was obtained by a low- 63

Received: March 16, 2020

Revised: April 16, 2020

Published: May 6, 2020

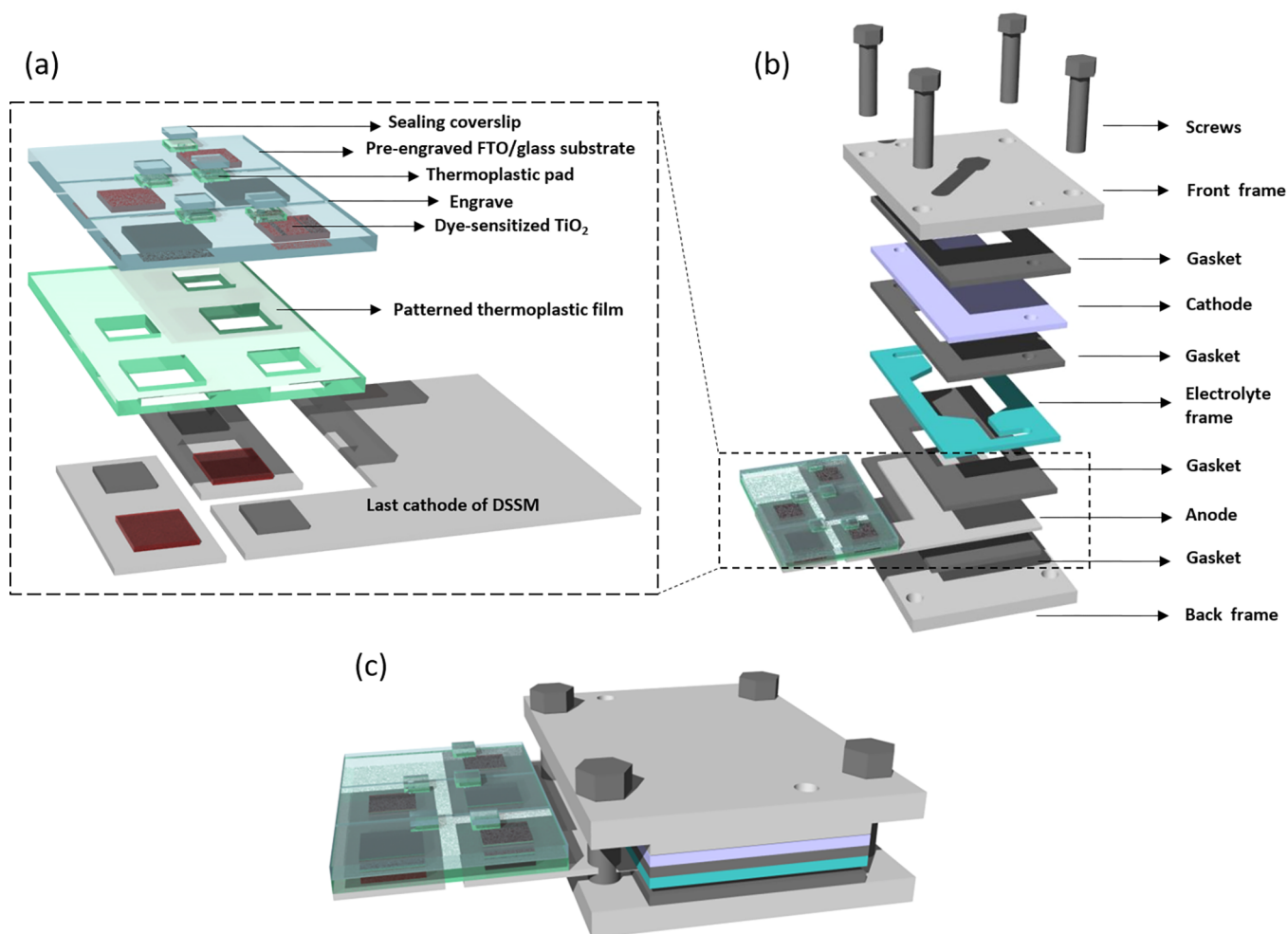


**Figure 1.** Scheme of the integrated PV–EC system: (a) solar module, (b) electrochemical reactor, and (c) integrated device.

64 cost all-Earth-abundant system, composed of a perovskite PV  
 65 minimodule and a two-chamber EC based on nanostructured  
 66 CuO for both the cathode and anode.<sup>17</sup> In all of the above-  
 67 mentioned and other works,<sup>14,15,18,19</sup> the PV cell/module is  
 68 coupled to the electrochemical reactor through electrical wire  
 69 connections, since the solar cell is external or attached to the  
 70 electrolyzer. In this sense, we can speak of connected systems,  
 71 but no real integrated systems (i.e., with shared electrodes  
 72 between the PV and the EC) have been proposed in the  
 73 literature so far.

74 In this work, we present, for the first time, an integrated  
 75 device for the solar-driven electrochemical conversion of CO<sub>2</sub>  
 76 to value-added products. To carry out the integration, we  
 77 concluded that a third-generation PV technology, namely, dye-  
 78 sensitized solar cell (DSSC), makes use of Pt as the cathodic  
 79 electrode;<sup>20</sup> at the same time, Pt is widely used as the anode  
 80 material in EC for CO<sub>2</sub> conversion.<sup>3,6,10</sup> With these premises,  
 81 we fabricated an integrated system in which the Pt electrode is  
 82 shared between the dye-sensitized solar module (DSSM) and  
 83 the electrochemical reactor, acting at the same time both as  
 84 cathode for the solar device and as anode for the EC. The  
 85 integrated system was able to carry out the unassisted CO<sub>2</sub>  
 86 reduction to CO under simulated solar irradiation for more  
 87 than 3 h.

## RESULTS AND DISCUSSION

88

The PV module is composed of five series-connected DSSCs, 89  
 similar to our previous work,<sup>21</sup> with an increase in the cell 90  
 number to five in order to achieve an operating voltage higher 91  
 than 2.5 V. The module employed a nanocrystalline TiO<sub>2</sub> 92  
 photoanode, Ru-based sensitizer, iodide/tri-iodide electrolyte, 93  
 and Pt cathode. Two different current collectors were selected 94  
 for module fabrication: transparent conductive substrate as the 95  
 front side (top of the device) and titanium foils as the back 96  
 side (bottom of the device). Details of the fabrication 97  
 procedure are reported in the [Supporting Information](#). The 98  
 dimension of the last cathode of the cell series was chosen in 99  
 order to overpass the PV module footprint and act as the 100  
 anode for the EC. Concerning the EC, a single-chamber 101  
 configuration was employed, in which no membrane was used 102  
 to separate the anode and the cathode, as shown in [Figure 1](#). 103 f1  
 This configuration has been adopted in order to reduce the 104  
 total cell overpotential by eliminating the proton exchange 105  
 membrane (see [Supporting Information](#) for details).<sup>11,22</sup> A 106  
 Cu–Sn electrocatalyst recently proposed by our group,<sup>23,24</sup> 107  
 characterized by a good selectivity toward CO, was used as the 108  
 cathodic material. The Cu–Sn cathode was prepared through a 109  
 cost-efficient electrodeposition route, as detailed in the 110  
[Supporting Information](#). The already mentioned Ti-supported 111  
 Pt was employed as the anode. A CO<sub>2</sub>-saturated 0.1 M 112  
 KHCO<sub>3</sub> aqueous solution was chosen as the electrolyte. The 113

114 volume of the electrolyte was 7 mL, with a 3 mL headspace. A  
 115 scheme of the integrated device is depicted in Figure 1.  
 116 The performance of the two components of the system was  
 117 first investigated individually. Figure 2 shows the current–

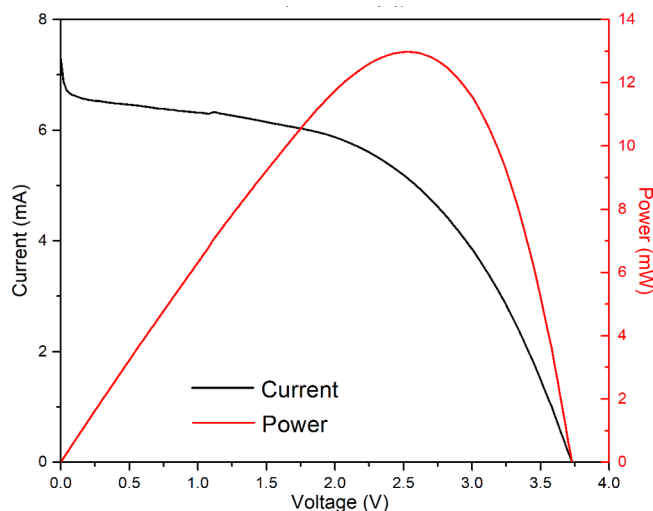


Figure 2. Current–voltage characteristic of the five-cell PV module under 1 sun illumination (left axis) and corresponding produced power (right axis).

118 voltage characteristic of the PV model acquired under AM1.5G  
 119 illumination. By comparing the curve in Figure 2 with the data  
 120 reported for our previously published DSSM,<sup>21</sup> it can be  
 121 observed that the addition of the fifth solar cell in the PV  
 122 module leads to a boost of the voltage with respect to the four-  
 123 cell module, with an open circuit value of 3.73 V, i.e., almost a  
 124 1 V increase. This improvement cannot be simply justified with  
 125 the addition of a cell since it is larger than the open circuit  
 126 voltage ( $V_{oc}$ ) of a traditional DSSC (based on the combination  
 127 of  $TiO_2$ , Ru-based dye and  $I^-/I_3^-$ ). Therefore, it must be  
 128 ascribed to the different architectures of the two DSSM.  
 129 Indeed, in the present study, Ti foils are used as current  
 130 collectors on one side of the module to allow integration with  
 131 the electrochemical reactor for  $CO_2$  reduction, while fluorine-  
 132 doped tin oxide (FTO)-coated glasses were used by Scalia et  
 133 al.<sup>21</sup> This variation induces two main effects: (i) the reduction  
 134 of the series resistance (accounting for the transport resistance  
 135 of the substrate) due to a higher conductivity of Ti with  
 136 respect to FTO and (ii) the *in situ* formation of a  $TiO_2$   
 137 blocking layer on the Ti surface during the thermal treatment  
 138 for photoanode preparation. While the former can influence  
 139 the photogenerated current, the latter can be considered as the  
 140 main reason responsible for the increased  $V_{oc}$  of the present  
 141 DSSM. In fact, it is well known that the introduction of a very  
 142 thin  $TiO_2$  layer between the current collector and the  
 143 nanostructured photoanode film allows for preventing electron  
 144 recombination with a positive effect on the  $V_{oc}$ .<sup>25</sup> For what  
 145 concerns the other parameters, both the PV modules exhibit  
 146 similar currents (short circuit value of about 7 mA) and fill  
 147 factors (0.48), thus leading to an enhanced photoconversion  
 148 efficiency of 2.68% for the novel five-cell device. It is worth  
 149 noting that a maximum power of 13 mW is produced by the  
 150 DSSM at 2.54 V and that power larger than 10 mW can be  
 151 obtained in the wide voltage range of 1.7–3.2 V.  
 152 The performance of the EC was assessed through 1 h  $CO_2$   
 153 electrolysis tests at different voltages. A micro-gas chromato-

graph ( $\mu GC$ ) was used for the online measurements of the  
 154 gaseous products, and a high-performance liquid chromato-  
 155 graph (HPLC) was used for the analysis of the liquid products  
 156 at the end of each test.<sup>26</sup> During the experiments, a constant  
 157  $CO_2$  flow of 10 mL/min was maintained in order to saturate  
 158 the electrolyte and to carry the gaseous products to the  $\mu GC$ .  
 159 Figure 3 reports the faradaic efficiency (FE) for the different  
 160 products

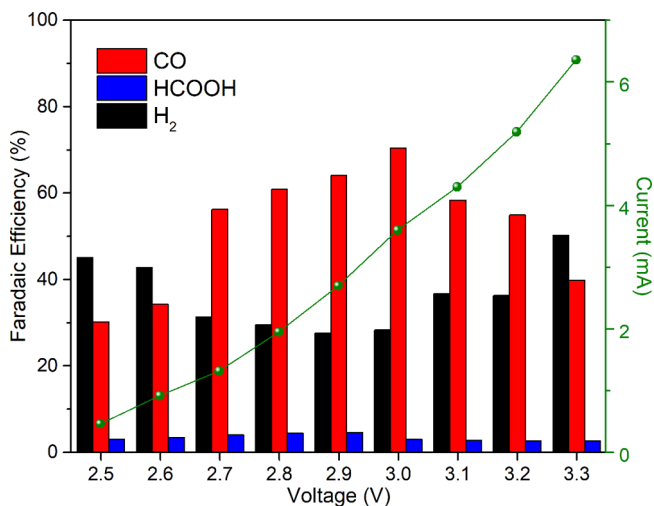
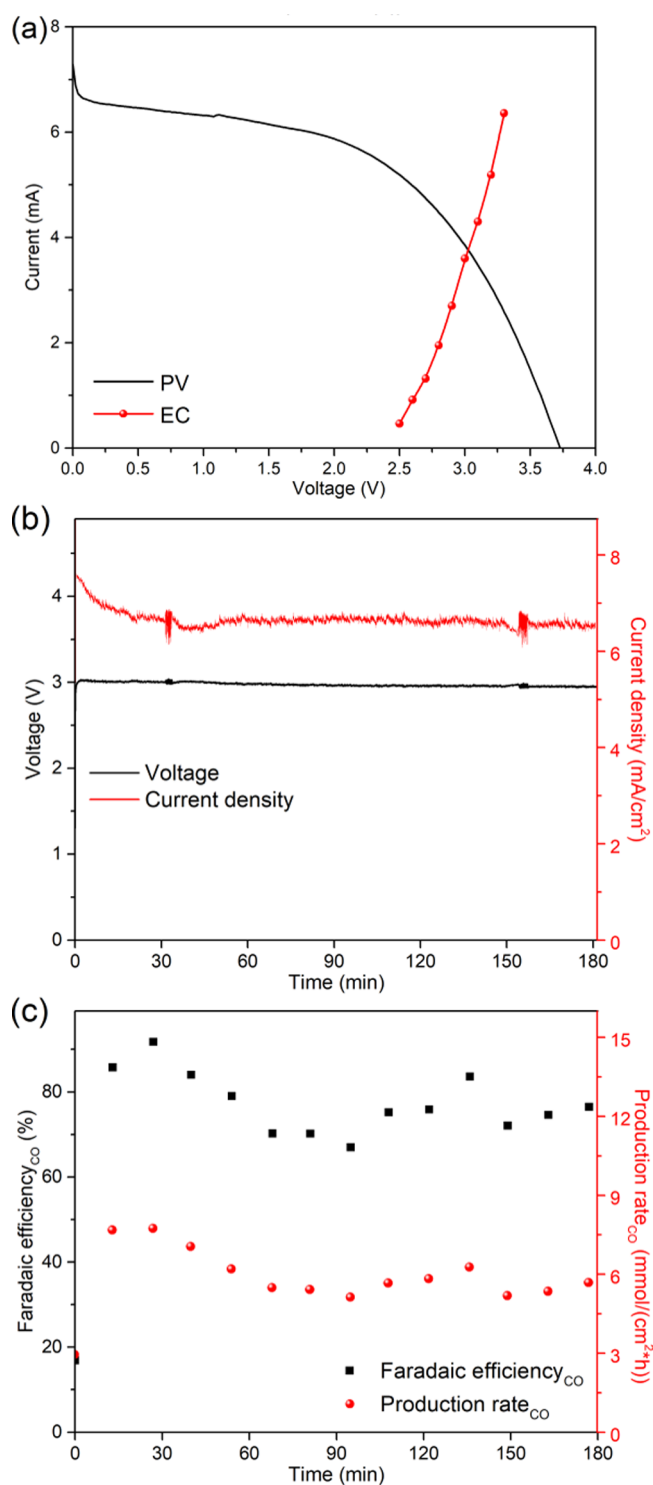


Figure 3. Faradaic efficiencies for  $CO$ ,  $HCOOH$ , and  $H_2$  formation in EC at various applied voltages during 1 h electrolysis (left axis) and corresponding measured currents (right axis).

161 reaction products as a function of the applied voltage. Only  
 162  $CO$  and  $H_2$  were detected as gaseous products, while just  
 163 formic acid ( $HCOOH$ ) was identified as the liquid product.  
 164 With the exception of low ( $\leq 2.6$  V) and high ( $\geq 3.3$  V)  
 165 voltages, the  $CO_2RR$  outperforms the competing hydrogen  
 166 evolution reaction, thus confirming the goodness of our Cu-  
 167 based electrocatalyst.<sup>23,24</sup> A maximum FE for  $CO$  production  
 168 of about 73% was obtained at 3.0 V, where the total measured  
 169 current is 3.6 mA (corresponding to a cathodic current density  
 170 of  $6.4 \text{ mA/cm}^2$ ). By comparing this data with those of the PV  
 171 module, an optimal operating point at 3.0 V can be envisaged  
 172 for the integrated system since the solar device produces a  
 173 similar current of 3.7 mA at this voltage.

174 Figure 4a shows the measured current–voltage characteristic  
 175 of the PV module under 1 sun illumination superimposed to  
 176 that of the EC. As anticipated above, the theoretical operating  
 177 point, given by the intersection of the two curves, can be found  
 178 at 3.0 V. At this potential, the power produced by the PV  
 179 module is 11.5 mW, and the partial current (density) for  $CO$   
 180 production is equal to 2.6 mA ( $4.7 \text{ mA/cm}^2$ ). The electrolysis  
 181 experiment on the integrated PV–EC system was carried out  
 182 under 1 sun illumination for more than 3 h, during which the  
 183 produced gases were measured by  $\mu GC$  (the liquid products  
 184 were measured after the test through HPLC). The results of  
 185 this measurement are reported in Figure 4b and c. The  
 186 integrated device is characterized by a constant voltage of  $3.00$   
 187  $\pm 0.06$  V for all the period of investigation and a by  
 188 corresponding stable current density equal to  $6.5 \pm 0.4 \text{ mA/}$   
 189  $\text{cm}^2$  after 30 min of operation (Figure 4b). It is worth noting  
 190 that such a stability is in line with or even better than those  
 191 reported for nonintegrated PV–EC systems.<sup>7,14,18</sup> In the initial  
 192 phase of the electrolysis, the decrease in the current density is  
 193 associated with the reduction of oxide species in the Cu–Sn



**Figure 4.** (a) Current–voltage characteristic of the five-cell PV module under 1 sun illumination and of the EC. (b) Voltage (left axis) and current density (right axis) during a 3 h test of the integrated PV–EC system under 1 sun illumination. (c) FE (left axis) and production rate (right axis) for CO during a 3 h test of the integrated PV–EC system under 1 sun illumination.

stable during 3 h of operation, thus proving that sunlight and  $\text{CO}_2$  can be efficiently and continuously converted by our integrated device, similarly to PV–EC coupled systems present in the literature.<sup>11,12,17</sup> A  $\text{CO}$  production rate of about 80 mmol/day (considering 24 h of continuous operation) was obtained along the 3 h test.

The obtained data was employed to calculate the solar-to- $\text{CO}$  efficiency  $\eta_{\text{STC}}$  of our integrated system, according to the formula

$$\eta_{\text{STC}} = \frac{E_{\text{CO}_2/\text{CO}}^0 \cdot J \cdot \text{FE}_{\text{CO}}}{W_{\text{sol}}} \quad (1)$$

where  $E_{\text{CO}_2/\text{CO}}^0$  is the standard cell potential when the EC conducts the  $\text{CO}_2$ RR to  $\text{CO}$  (equal to 1.34 V),  $J$  is the current density of the PV module,  $\text{FE}_{\text{CO}}$  is the faradaic efficiency for  $\text{CO}$ , and  $W_{\text{sol}}$  is the solar irradiance.<sup>11</sup> A solar-to- $\text{CO}$  efficiency equal to 0.79% is found for our integrated PV–EC system. This efficiency can be further increased considering also  $\text{H}_2$  as a secondary product (for example, for the production of syngas),<sup>27</sup> leading to a total solar-to-fuel efficiency of 0.97%. The obtained values are comparable to the efficiencies presented in the literature for coupled PV–EC systems.<sup>14</sup> Better results have been also reported.<sup>11,17,18</sup> However, it has to be highlighted that the performance of our integrated PV–EC system can be improved since different aspects can be optimized:

- An additional PV cell can be added to the module in order to enlarge the voltage window of the module and shift the operating point in a region of higher cell efficiency.
- Adapting the active area of the PV module to the electrocatalyst one can be done in order to match the two currents.

These aspects have already been taken into consideration in a new work which is in progress in our lab. Nevertheless, the present work demonstrates the feasibility of an integrated PV–EC system that enables the solar-driven electrochemical conversion of  $\text{CO}_2$ .

## CONCLUSION

An integrated system composed of a third-generation PV module and an EC for the electroreduction of  $\text{CO}_2$  under solar illumination has been presented here. The PV module is based on a series of five DSSCs, while the EC is based on a Cu–Sn electrocatalyst. The integration of the two devices has been achieved through a common Pt-based electrode, which works both as a cathode for the PV module and as an anode for the EC.

A stable voltage of 3 V has been obtained from the integrated system under 1 sun illumination for 3 h, during which  $\text{CO}$  production with a FE of 78% was achieved as a result of the unassisted  $\text{CO}_2$ RR. This represents the first integrated artificial photosynthesis device for the solar-driven electrochemical conversion of  $\text{CO}_2$ . This system is currently under optimization in our laboratory in order to improve the overall device efficiency.

## ASSOCIATED CONTENT

### Supporting Information

The Supporting Information is available free of charge at <https://pubs.acs.org/doi/10.1021/acssuschemeng.0c02088>.

cathode.<sup>23,24</sup> In accordance with the analysis conducted on the bare EC, only  $\text{CO}$  and  $\text{HCOOH}$  were detected as  $\text{CO}_2$ RR products, with average FE values equal to about 78% and 2%, respectively. The FE for  $\text{CO}$  is plotted as a function of the electrolysis time in Figure 4c. It can be observed that it remains

256 Experimental section, measurements of membrane  
257 overpotential, scheme of DSSM, scheme of EC, and  
258 pictures of the integrated PV–EC device (PDF)

## 259 ■ AUTHOR INFORMATION

### 260 Corresponding Authors

261 **Adriano Sacco** – Center for Sustainable Future Technologies @  
262 Polito, Istituto Italiano di Tecnologia, 10144 Torino, Italy;

263 [orcid.org/0000-0002-9229-2113](https://orcid.org/0000-0002-9229-2113); Phone: +39 011

264 5091912; Email: [adriano.sacco@iit.it](mailto:adriano.sacco@iit.it); Fax: +39 011

265 5091901

266 **Andrea Lamberti** – Center for Sustainable Future Technologies  
267 @Polito, Istituto Italiano di Tecnologia, 10144 Torino, Italy;

268 Applied Science and Technology Department, Politecnico di  
269 Torino, Corso Duca degli Abruzzi, 10129 Torino, Italy;

270 [orcid.org/0000-0003-4100-9661](https://orcid.org/0000-0003-4100-9661); Phone: +39 011

271 0907394; Email: [andrea.lamberti@polito.it](mailto:andrea.lamberti@polito.it); Fax: +39 011

272 0907399

### 273 Authors

274 **Roberto Speranza** – Center for Sustainable Future Technologies  
275 @Polito, Istituto Italiano di Tecnologia, 10144 Torino, Italy;

276 Applied Science and Technology Department, Politecnico di  
277 Torino, Corso Duca degli Abruzzi, 10129 Torino, Italy

278 **Umberto Savino** – Center for Sustainable Future Technologies  
279 @Polito, Istituto Italiano di Tecnologia, 10144 Torino, Italy;

280 Applied Science and Technology Department, Politecnico di  
281 Torino, Corso Duca degli Abruzzi, 10129 Torino, Italy

282 **Juqin Zeng** – Center for Sustainable Future Technologies @  
283 Polito, Istituto Italiano di Tecnologia, 10144 Torino, Italy

284 **M. Amin Farkhondehfal** – Center for Sustainable Future  
285 Technologies @Polito, Istituto Italiano di Tecnologia, 10144  
286 Torino, Italy

287 **Angelica Chiodoni** – Center for Sustainable Future  
288 Technologies @Polito, Istituto Italiano di Tecnologia, 10144  
289 Torino, Italy

290 **Candido F. Pirri** – Center for Sustainable Future Technologies  
291 @Polito, Istituto Italiano di Tecnologia, 10144 Torino, Italy;

292 Applied Science and Technology Department, Politecnico di  
293 Torino, Corso Duca degli Abruzzi, 10129 Torino, Italy

294 Complete contact information is available at:

295 <https://pubs.acs.org/10.1021/acssuschemeng.0c02088>

### 296 Author Contributions

297 The manuscript was written through contributions of all  
298 authors. All authors have given approval to the final version of  
299 the manuscript.

### 300 Notes

301 The authors declare no competing financial interest.

## 302 ■ REFERENCES

303 (1) Saracco, G.; Vankova, S.; Pagliano, C.; Bonelli, B.; Garrone, E.  
304 Outer Co(II) Ions in Co-ZIF-67 Reversibly Adsorb Oxygen from  
305 Both Gas Phase and Liquid Water. *Phys. Chem. Chem. Phys.* **2014**, *16*,  
306 6139–6145.

307 (2) Hernández, S.; Tortello, M.; Sacco, A.; Quaglio, M.; Meyer, T.;  
308 Bianco, S.; Saracco, G.; Pirri, C. F.; Tresso, E. New Transparent  
309 Laser-Drilled Fluorine-Doped Tin Oxide Covered Quartz Electrodes  
310 for Photo-Electrochemical Water Splitting. *Electrochim. Acta* **2014**,  
311 *131*, 184–194.

312 (3) Sacco, A. Electrochemical Impedance Spectroscopy as a Tool to  
313 Investigate the Electroreduction of Carbon Dioxide: A Short Review.  
314 *J. CO<sub>2</sub> Util.* **2018**, *27*, 22–31.

(4) Bushuyev, O. S.; De Luna, P.; Dinh, C. T.; Tao, L.; Saur, G.; van  
de Lagemaat, J.; Kelley, S. O.; Sargent, E. H. What Should We Make  
with CO<sub>2</sub> and How Can We Make It? *Joule* **2018**, *2*, 825–832.

(5) Sacco, A.; Zeng, J.; Bejtka, K.; Chiodoni, A. Modeling of Gas  
Bubble-Induced Mass Transport in the Electrochemical Reduction of  
Carbon Dioxide on Nanostructured Electrodes. *J. Catal.* **2019**, *372*,  
39–48.

(6) Farkhondehfal, M. A.; Hernández, S.; Rattalino, M.; Makkee, M.;  
Lamberti, A.; Chiodoni, A.; Bejtka, K.; Sacco, A.; Pirri, C. F.; Russo,  
N. Syngas Production by Electrocatalytic Reduction of CO<sub>2</sub> Using  
Ag-Decorated TiO<sub>2</sub> Nanotubes. *Int. J. Hydrogen Energy* **2019**, *na*, na  
DOI: 10.1016/j.ijhydene.2019.04.180.

(7) Zhou, X.; Liu, R.; Sun, K.; Chen, Y.; Verlage, E.; Francis, S. A.;  
Lewis, N. S.; Xiang, C. Solar-Driven Reduction of 1 Atm of CO<sub>2</sub> to  
Formate at 10% Energy-Conversion Efficiency by Use of a TiO<sub>2</sub>-  
Protected III-V Tandem Photoanode in Conjunction with a Bipolar  
Membrane and a Pd/C Cathode. *ACS Energy Lett.* **2016**, *1*, 764–770.

(8) Liang, L.; Lei, F.; Gao, S.; Sun, Y.; Jiao, X.; Wu, J.; Qamar, S.;  
Xie, Y. Single Unit Cell Bismuth Tungstate Layers Realizing Robust  
Solar CO<sub>2</sub> Reduction to Methanol. *Angew. Chem., Int. Ed.* **2015**, *54*,  
13971–13974.

(9) Asadi, M.; Kim, K.; Liu, C.; Addepalli, A. V.; Abbasi, P.; Yasaei,  
P.; Phillips, P.; Behranginia, A.; Cerrato, J. M.; Haasch, R.; Zapol, P.;  
Kumar, B.; Klie, R. F.; Abiade, J.; Curtiss, L. A.; Salehi-Khojin, A.  
Nanostructured Transition Metal Dichalcogenide Electrocatalysts for  
CO<sub>2</sub> Reduction in Ionic Liquid. *Science* **2016**, *353*, 467–470.

(10) Kauffman, D. R.; Thakkar, J.; Siva, R.; Matranga, C.;  
Ohodnicki, P. R.; Zeng, C.; Jin, R. Efficient Electrochemical CO<sub>2</sub>  
Conversion Powered by Renewable Energy. *ACS Appl. Mater.*  
*Interfaces* **2015**, *7*, 15626–15632.

(11) Schreier, M.; Curvat, L.; Giordano, F.; Steier, L.; Abate, A.;  
Zakeeruddin, S. M.; Luo, J.; Mayer, M. T.; Grätzel, M. Efficient  
Photosynthesis of Carbon Monoxide from CO<sub>2</sub> Using Perovskite  
Photovoltaics. *Nat. Commun.* **2015**, *6*, 7326.

(12) Schreier, M.; Héroguel, F.; Steier, L.; Ahmad, S.; Luterbacher, J.  
S.; Mayer, M. T.; Luo, J.; Grätzel, M. Solar Conversion of CO<sub>2</sub> to CO  
Using Earth-Abundant Electrocatalysts Prepared by Atomic Layer  
Modification of CuO. *Nat. Energy* **2017**, *2*, 17087.

(13) White, J. L.; Herb, J. T.; Kaczur, J. J.; Majsztrik, P. W.; Bocarsly,  
A. B. Photons to Formate: Efficient Electrochemical Solar Energy  
Conversion Via Reduction of Carbon Dioxide. *J. CO<sub>2</sub> Util.* **2014**, *7*,  
1–5.

(14) Ren, D.; Loo, N. W. X.; Gong, L.; Yeo, B. S. Continuous  
Production of Ethylene from Carbon Dioxide and Water Using  
Intermittent Sunlight. *ACS Sustainable Chem. Eng.* **2017**, *5*, 9191–  
9199.

(15) Sriramagiri, G. M.; Ahmed, N.; Luc, W.; Dobson, K. D.;  
Hegedus, S. S.; Jiao, F. Toward a Practical Solar-Driven CO<sub>2</sub> Flow  
Cell Electrolyzer: Design and Optimization. *ACS Sustainable Chem.*  
*Eng.* **2017**, *5*, 10959–10966.

(16) Gurudayal; Bullock, J.; Srankó, D. F.; Towle, C. M.; Lum, Y.;  
Hettick, M.; Scott, M. C.; Javey, A.; Ager, J. Efficient Solar-Driven  
Electrochemical CO<sub>2</sub> Reduction to Hydrocarbons and Oxygenates.  
*Energy Environ. Sci.* **2017**, *10*, 2222–2230.

(17) Huan, T. N.; Dalla Corte, D. A.; Lamaison, S.; Karapinar, D.;  
Lutz, L.; Menguy, N.; Foldyna, M.; Turren-Cruz, S.-H.; Hagfeldt, A.;  
Bella, F.; Fontecave, M.; Mougél, V. Low-Cost High-Efficiency  
System for Solar-Driven Conversion of CO<sub>2</sub> to Hydrocarbons. *Proc.*  
*Natl. Acad. Sci. U. S. A.* **2019**, *116*, 9735–9740.

(18) Urbain, F.; Tang, P.; Carretero, N. M.; Andreu, T.; Gerling, L.  
G.; Voz, C.; Arbiol, J.; Morante, J. R. A Prototype Reactor for Highly  
Selective Solar-Driven CO<sub>2</sub> Reduction to Synthesis Gas Using  
Nanosized Earth-Abundant Catalysts and Silicon Photovoltaics.  
*Energy Environ. Sci.* **2017**, *10*, 2256–2266.

(19) Sugano, Y.; Ono, A.; Kitagawa, R.; Tamura, J.; Yamagiwa, M.;  
Kudo, Y.; Tsutsumi, E.; Mikoshiba, S. Crucial Role of Sustainable  
Liquid Junction Potential for Solar-to-Carbon Monoxide Conversion  
by a Photovoltaic Photoelectrochemical System. *RSC Adv.* **2015**, *5*,  
54246–54252.

- 384 (20) Sacco, A. Electrochemical Impedance Spectroscopy: Funda-  
385 mentals and Application in Dye-Sensitized Solar Cells. *Renewable*  
386 *Sustainable Energy Rev.* **2017**, *79*, 814–829.
- 387 (21) Scalia, A.; Varzi, A.; Lamberti, A.; Tresso, E.; Jeong, S.; Jacob,  
388 T.; Passerini, S. High Energy and High Voltage Integrated Photo-  
389 Electrochemical Double Layer Capacitor. *Sustain. Energy Fuels* **2018**,  
390 *2*, 968–977.
- 391 (22) Singh, M. R.; Clark, E. L.; Bell, A. T. Effects of Electrolyte,  
392 Catalyst, and Membrane Composition and Operating Conditions on  
393 the Performance of Solar-Driven Electrochemical Reduction of  
394 Carbon Dioxide. *Phys. Chem. Chem. Phys.* **2015**, *17*, 18924–18936.
- 395 (23) Zeng, J.; Bejtka, K.; Ju, W.; Castellino, M.; Chiodoni, A.; Sacco,  
396 A.; Farkhondehfar, M. A.; Hernández, S.; Rentsch, D.; Battaglia, C.;  
397 Pirri, C. F. Advanced Cu-Sn Foam for Selectively Converting CO<sub>2</sub> to  
398 CO in Aqueous Solution. *Appl. Catal., B* **2018**, *236*, 475–482.
- 399 (24) Ju, W.; Zeng, J.; Bejtka, K.; Ma, H.; Rentsch, D.; Castellino, M.;  
400 Sacco, A.; Pirri, C. F.; Battaglia, C. Sn-Decorated Cu for Selective  
401 Electrochemical CO<sub>2</sub> to CO Conversion: Precision Architecture  
402 Beyond Composition Design. *ACS Appl. Energy Mater.* **2019**, *2*, 867–  
403 872.
- 404 (25) Bella, F.; Sacco, A.; Pugliese, D.; Laurenti, M.; Bianco, S.  
405 Additives and Salts for Dye-Sensitized Solar Cells Electrolytes: What  
406 Is the Best Choice? *J. Power Sources* **2014**, *264*, 333–343.
- 407 (26) Bejtka, K.; Zeng, J.; Sacco, A.; Castellino, M.; Hernández, S.;  
408 Farkhondehfar, M. A.; Savino, U.; Ansaloni, S.; Pirri, C. F.; Chiodoni,  
409 A. Chainlike Mesoporous SnO<sub>2</sub> as a Well-Performing Catalyst for  
410 Electrochemical CO<sub>2</sub> Reduction. *ACS Appl. Energy Mater.* **2019**, *2*,  
411 3081–3091.
- 412 (27) Zeng, J.; Bejtka, K.; Di Martino, G.; Sacco, A.; Castellino, M.;  
413 Re Fiorentin, M.; Risplendi, F.; Farkhondehfar, M. A.; Hernández, S.;  
414 Cicero, G.; Pirri, C. F.; Chiodoni, A. Microwave-Assisted Synthesis of  
415 Copper-Based Electrocatalysts for Converting Carbon Dioxide to  
416 Tunable Syngas. *ChemElectroChem* **2020**, *7*, 229–238.